



Published in final edited form as:

Dev Biol. 2022 November ; 491: 43–55. doi:10.1016/j.ydbio.2022.08.010.

TRIM-NHL protein, NHL-2, modulates cell fate choices in the *C. elegans* germ line

John L. Brenner^a, Erin M. Jyo^b, Ariz Mohammad^a, Paul Fox^a, Vovanti Jones^a, Elaine Mardis^c, Tim Schedl^{a,**}, Eleanor M. Maine^{b,*}

^aDepartment of Genetics, Washington University School of Medicine, St. Louis, MO, 63110, USA

^bDepartment of Biology, Syracuse University, Syracuse, NY, 13210, USA

^cMcDonnell Genome Institute, Washington University School of Medicine, St. Louis, MO, 63110, USA

Abstract

Many tissues contain multipotent stem cells that are critical for maintaining tissue function. In *Caenorhabditis elegans*, germline stem cells allow gamete production to continue in adulthood. In the gonad, GLP-1/Notch signaling from the distal tip cell niche to neighboring germ cells activates a complex regulatory network to maintain a stem cell population. GLP-1/Notch signaling positively regulates production of LST-1 and SYGL-1 proteins that, in turn, interact with a set of PUF/FBF proteins to positively regulate the stem cell fate. We previously described *sog* (suppressor of *glp-1* loss of function) and *teg* (tumorous enhancer of *glp-1* gain of function) genes that limit the stem cell fate and/or promote the meiotic fate. Here, we show that *sog-10* is allelic to *nhl-2*. NHL-2 is a member of the conserved TRIM-NHL protein family whose members can bind RNA and ubiquitinate protein substrates. We show that NHL-2 acts, at least in part, by inhibiting the expression of PUF-3 and PUF-11 translational repressor proteins that promote the stem cell fate. Two other negative regulators of stem cell fate, CGH-1 (conserved germline helicase) and ALG-5 (Argonaute protein), may work with NHL-2 to modulate the stem cell population. In addition, NHL-2 activity promotes the male germ cell fate in XX animals.

Keywords

C. elegans; Germline; Stem cell fate; GLP-1/Notch signaling; TRIM-NHL proteins; NHL-2

1. Introduction

Formation of specialized cells during animal development involves a series of tightly regulated cell fate choices. Many tissues contain stem cells, which retain the ability to

This is an open access article under the CC BY-NC-ND license (<http://creativecommons.org/licenses/by-nc-nd/4.0/>).

*Corresponding author. emmaine@syr.edu (E.M. Maine). **Corresponding author. ts@wustl.edu (T. Schedl).

Declarations of competing interest

None.

Appendix A. Supplementary data

Supplementary data to this article can be found online at <https://doi.org/10.1016/j.ydbio.2022.08.010>.

self-renew or give rise to cells with a more limited fate. An example is germline stem cells (GSCs) in the nematode, *Caenorhabditis elegans* (reviewed by Hubbard and Schedl, 2019). The *C. elegans* gonad is organized as a reflexed tube with mitotically cycling stem cells located at the distal end and mature gametes accumulating at the proximal end. The somatic distal tip cell (DTC) surrounds the distal end of the germ line and provides a niche, communicating with germ cells via Notch-type signaling to specify the stem cell fate and prevent those cells from entering meiosis (Fig. 1). The germline expresses a Notch-type receptor called GLP-1, so named because mutants have a germline proliferation defective phenotype (Austin and Kimble, 1987). Immediately proximal to the GSCs is a population of cells completing a final mitotic cell cycle, and further proximal is a population of non-cycling cells in meiotic S phase (Hansen et al. 2004; Crittenden et al. 2006; Maciejowski et al. 2006; Jaramillo-Lambert et al. 2007; Fox et al. 2011; Fox and Schedl, 2015; Seidel and Kimble, 2015). These three populations are collectively called the progenitor zone. As cells complete meiotic S phase and move further proximally away from the niche, they enter meiotic prophase I under control of several meiotic entry pathways. When GLP-1/Notch signaling is impaired, some or all germline stem cells will prematurely exit mitosis and enter meiosis, indicating that this signaling maintains the GSC fate. Hence, the *glp-1* loss of function phenotype is a premature switch from stem cell fate to meiotic fate. Although GLP-1/Notch signaling maintains the GSC population, it is important to note that it does not appear to regulate the frequency or length of mitotic cycling in these cells.

A network of factors acts downstream of GLP-1 to regulate cell fate in the distal germ line. GLP-1/Notch signaling directly upregulates transcription of two genes, *lst-1* and *sygl-1*, whose protein products act together with four PUF (Pumilio and EBF) family mRNA-binding proteins, FBF-1 (*fem-3* binding factor), FBF-2, PUF-3, and PUF-11, to promote the GSC fate (Kershner et al. 2014; Lee et al., 2016; Brenner and Schedl, 2016; Shin et al., 2017; Haupt et al. 2019, 2020; Chen et al. 2020). LST-1/PUF and SYGL-1/PUF regulatory complexes are thought to act by upregulating production of factors necessary to maintain the GSC fate and/or downregulating production of factors necessary for meiotic entry.

The cumulative action of several other factors, in addition to GLP-1/Notch signaling, modulates the distal progenitor pool while allowing the steady entry of germ cells into meiosis. These include physiologically important inputs, e.g., insulin-like signaling, that promote mitotic cell proliferation, and hence progenitor zone size, but do not promote the GSC fate (Michaelson et al. 2010). Complicating the analysis, some factors that regulate the GSC fate decision have an independent function that effects progenitor zone size, for example a role in mitotic cell cycling. This is illustrated by *puf-8* that inhibits the GSC fate and/or promotes meiotic entry, but, counterintuitively, also promotes the normal sized progenitor zone through a function in mitotic cell cycle progression, which was revealed through a genetic interaction with *mex-3* (Racher and Hansen, 2012; Ariz et al. 2009).

One important approach for identifying factors that regulate GSC fate versus meiotic development has been to conduct genetic screens in a sensitized background where *glp-1* activity is either partially reduced or mildly elevated compared to wildtype (reviewed in Hubbard and Schedl, 2019). Factors that promote the GSC fate have been identified in

screens for enhancers of the premature meiotic entry phenotype associated with a partial loss of *glp-1* function. In contrast, factors that promote meiotic entry have been identified in screens for suppressors of a weak Glp-1 loss of function phenotype or enhancers of the excess, mitotically cycling stem cells (a germline tumor) associated with a weak Glp-1 gain--of-function phenotype. These genetic approaches have identified numerous factors, although in many cases it is not yet known how they intersect with the GSC gene regulatory network (Fig. 1).

A single allele of *sog-10* (suppressor of *glp-1*), *sog-10(q162)*, was previously described as influencing two cell fate choices in the *C. elegans* germline: GSC fate vs meiotic development, and male (sperm) vs female (oocyte) gametogenesis (Maine and Kimble, 1993). As evidence that *sog-10* influences the GSC vs meiotic choice, *sog-10(q162)* suppresses a partial loss of GLP-1/Notch signaling in the germ line, indicating a greater number of cells are choosing the GSC fate. As evidence that *sog-10* influences the germline male vs female fate choice, some *sog-10(q162)* hermaphrodites produce only oocytes when raised at low temperatures, indicating that larval germ cells fail to choose the male fate. Here, we report that *q162* is a loss-of-function mutation in the *nhl-2* gene. NHL-2 is a TRIM-NHL protein expressed in the soma and germ line, and it is implicated in regulating gene expression at multiple post-transcriptional levels (Hyenne et al., 2008; McJunkin and Ambros, 2017; Davis et al. 2018). TRIM-NHL proteins function in diverse animal species where they regulate developmental fate choices (Tocchini and Ciosk, 2015; Connacher and Goldstrohm, 2021). Characteristic features of this protein family are (i) a TRIPartite Motif (TRIM), comprising a RING domain, B-Box-type zinc fingers, and a coiled-coil domain that functions in ubiquitinating target proteins, and (ii) a C-terminal NHL domain with RNA-binding capability (Hyenne et al. 2008; Tocchini and Ciosk, 2015; Connacher and Goldstrohm, 2021). We identify distinct germline-autonomous functions for NHL-2 in two fate choices: limiting the GSC fate and/or promoting differentiation (meiotic entry), at least in part through inhibition of PUF-3 and PUF-11 accumulation; and promoting the male germ cell fate in the larval XX hermaphrodite germline. We identify two other negative regulators of the GSC fate, CGH-1 (conserved germline helicase) and ALG-5 (argonaute-like gene), that may work with NHL-2 to regulate the GSC vs meiotic choice.

2. Materials and Methods

2.1. Genetics

Strains were cultured using standard methods. The *C. elegans* Bristol variant (N2) and mutations used are listed in Wormbase or described in the text.

The following mutations were used. LG (linkage group) I: *alg-5(tm1163)*, *alg-5(gk119870)*, *alg-5(gk870731)*, *gld-1(q485)*, *gld-2(q497)*, *rrf-1(pk1417)*. LGII: *fbf-1(ok91)*, *fbf-2(q704)*, *gld-3(q730)*, *nos-3(oz231)*. LGIII: *cgh-1(ok492)*, *dpy-17(e164)*, *glp-1(q224ts)*, *glp-1(ar202gf)*, *glp-1(oz264gf)*, *nhl-2(ok818)*, *pal-1(ct224)*, *sog-10(q162)*, *unc-32(e189)*. LGV: *rde-1(ne219)*. We used the GFP-expressing balancers *hT2[bli-4(e937) let-?(q782) qIs48]* and *mIn1[dpy-10(e128) mIs14]*. CRISPR-Cas9 gene-edited *lst-1::3xflag* and *3xflag::sygl-1* are described in Kocsisova et al. (2019), and *3xV5::puf-3* and *3xV5::puf-11* are described in Haupt et al. (2020). A strain expressing germline *rde-1(+)* is

described below (Marré et al., 2016). We use the abbreviation (*0*) to designate the canonical null allele of a gene, and otherwise specify the allele used.

2.2. Whole genome sequencing

Genomic DNA isolation from *sog-10(q162)* homozygous mutants, library construction, whole genome sequencing (WGS), and bioinformatics analysis were performed as described (Rastogi et al. 2015). 3-factor mapping prior to WGS placed *q162* within the *pal-1 – dpy-17* interval on LGIII. Therefore, we particularly focused on WGS data from this region. Two coding changes were detected in the *pal-1 – dpy-17* interval and three coding changes were detected in nearby flanking regions (Fig. 1A). These coding changes were as follows: open reading frame (ORF) B0285.4, nucleotide (nt) 4345012 G→T, amino acid (aa) A→S; *him-18/T04A8.15*, nt 4712954 C→G, aa W→C; *fkf-5/F26A1.2*, nt 4845218 A→T, aa N→I; *nhl-2/F26F4.7*, nt 4896956 C→T, aa W→stop; and K10D2.1, nt 5195035 C→A, aa T→K.

2.3. RNAi

RNAi was performed by the standard feeding method adapted from Timmons et al. (2001). *glp-1(+)* or *glp-1(q224ts)*L1 animals at 20 °C were fed single *E. coli* strains containing bacterial plasmids expressing dsRNA corresponding to candidate genes in the mapped LGIII interval, and then scored as adults. Germline-specific RNAi was performed with a strain that expresses RDE-1, an Argonaute protein required for RNAi, under a germline *mex-5* promoter (*mex-5p::rde-1(+); rde-1(ne219)*) (Marré et al., 2016). In addition, RNAi experiments were also performed in a *rrf-1(0)* background where RNAi is disabled in many somatic tissues, including the somatic gonad (Kumsta and Hansen, 2012).

2.4. Embryo assays

Embryo counts were obtained by standard methods. Temperature-sensitive *glp-1(q224)*, *nhl-2(q162) glp-1(q224)*, *nhl-2(ok818) glp-1(q224)*, and *alg-5(tm1163); glp-1(q224)* strains were maintained at 15 °C. To assay for embryo production, L1 larvae were picked to individual 20 °C plates and maintained at 20 °C throughout the experiment. If individuals developed as gravid adults, they were moved to fresh plates daily, and embryos present on the plates were counted. Plates were checked 1 and 2 days later to determine if any embryos hatched as larvae. *alg-5(tm1163); nhl-2(ok818) glp-1(q224)* individuals were very unhealthy, particularly at 15 °C. Therefore, a balanced *alg-5(tm1163)/hT2 gfp; nhl-2(ok818) glp-1(q224)/hT2 gfp* strain was maintained at 20 °C. Homozygous, maternally rescued, *alg-5(tm1163); nhl-2(ok818) glp-1(q224)* individuals were obtained for the embryo assay.

2.5. Immunocytochemistry

Antibodies were kindly provided by the following colleagues: anti-NHL-2 from the Labbe lab; anti-HIM-3 from the Zetka lab; anti-REC-8 from the Jantch/Loidl lab; and anti-MSP from the Greenstein lab. Anti-V5-Tag antibody was purchased from Bio-Rad, anti-WAPL-1 from Novus, and anti-FLAG M2 monoclonal from Sigma. REC-8 or WAPL-1 staining were used to identify progenitor zone cells and determine length of the zone, while HIM-3 staining was used to identify cells that had entered meiotic prophase (Hubbard and Schedl,

2019). Immunostaining was performed as described: anti-NHL-2 (Hyenne et al., 2008), anti-REC-8 (Fox et al. 2011), anti-WAPL-1 (Mohammad et al. 2018), and anti-MSP labeling (Kosinski et al. 2005). The anti-FLAG labeling protocol was adapted from Kocsisova et al. (2019). The anti-HIM-3 labeling protocol was adapted from She et al. (2009). 3xV5::PUF-3 and 3xV5::PUF-11 images were quantified as described (Baudrimont et al. 2022). DAPI staining and anti-HIM-3 labeling of *fbf-1(0) fbf-2(0); nhl-2(ok818)* and controls were done with strains carrying *unc-32(e189)* as a marker, e.g., *nhl-2(ok818) unc-32(e189)* and *fbf-1(0) fbf-2(0); nhl-2(ok818) unc-32(e189)*, in addition to N2 wildtype controls. LST-1::3xFLAG and 3xFLAG::SYGL-1 images were captured as Z-stacks on a Leica DM5500 upright microscope using a Hamamatsu ORCA-R2 camera and processed by deconvolution. Signal was quantified by analyzing maximum projection images with Plot Profile Analysis in ImageJ/FIJI using a method adapted from Haupt et al. (2020).

To quantify anti-V5::PUF-X labeling, wildtype N2 germlines were co-incubated with anti-V5 to identify non-specific signal, and this signal was then removed from images of V5-tagged germlines. *3xV5::puf-X* strains were dissected separately, while N2 and *3xV5::puf-X; nhl-2(ok818)* were dissected together. All the gonads were stained with anti-WAPL-1 and anti-V5 antibodies. In addition, to distinguish gonads of different genotype while capturing images, some tissue was stained with pSUN-1 antibody. For replicates 1 and 3, *3xV5::puf-X* were also stained with pSUN-1 antibody; for replicates 2 and 4, N2 and *3xV5::puf-X; nhl-2(ok818)* were also stained with pSUN-1 antibody. After primary antibody incubation, separately labeled 3xV5::PUF-X and N2 + 3xV5::PUF-X; *nhl-2(ok818)* were mixed together in the same tube and were further subjected to secondary antibody staining and processing. Hyperstack images were captured using a spinning disk confocal microscope (PerkinElmer-Cetus, Norwalk, CT). Exposure time for each channel was kept constant for an individual experiment. Two overlapping Hyperstack images were captured to get a coverage of ~50 cd from the distal end of the gonad. The images were further processed in Fiji, and DAPI-stained nuclei were used to mark the cell diameters (cds). Starting at the distal end, cd-wise plot profiles (intensity) were extracted by using custom python script for each gonad and were stored in text files. The intensity data were processed in R (<https://cran.r-project.org>) to visualize protein levels. WAPL-1 staining was used for the estimation of the progenitor zone length. All the scripts related to image processing and data analysis can be found at github (<https://github.com/arizmohammad>).

3. Results

3.1. *sog-10(q162)* is allelic to *nhl-2*

The *sog-10(q162)* mutation partially suppresses the premature meiotic entry phenotype of *glp-1* partial loss-of-function (*lf*) mutations (Maine and Kimble, 1993). It is unique among described *sog* mutations in that it does not suppress the *glp-1(lf)* embryonic lethal phenotype. We set out to identify the causative mutation in *q162*. Traditional three-point mapping placed *q162* in a region on LGIII between *pal-1* and *dpy-17*. Whole genome sequencing revealed five coding region mutations within or near the *pal-1* to *dpy-17* region (Fig. 2A) (see Methods). We assayed for suppression of the premature meiotic entry phenotype by knocking down these five genes individually by RNAi in *glp-1(q224)*

animals cultured at 20 °C. At 20 °C, the wildtype hermaphrodite germline produces ~300 sperm during larval development before switching to oogenesis at the adult molt and subsequently producing embryos. The *glp-1(q224)* mutation is temperature-sensitive (*ts*); when mutant hermaphrodites are raised at 20 °C, their germ cell precursors all enter meiosis prematurely and undergo spermatogenesis, and hence these animals do not produce oocytes or embryos. We asked whether RNAi-mediated knockdown of any of the five candidate *sog-10* genes could suppress the *glp-1(q224)* meiotic entry defect sufficiently to allow production of embryos. Among the five genes tested, only knockdown of *nhl-2* resulted in suppression, where *glp-1(q224)* hermaphrodites produced embryos at 20 °C. These *nhl-2(RNAi) glp-1(q224)* embryos did not hatch, indicating the *glp-1(lf)* embryonic lethality was not suppressed by *nhl-2(RNAi)*.

The *nhl-2* coding sequence isolated from the *q162* strain contains a C to T transition that changes a tryptophan residue to a premature stop codon in exon 5, approximately halfway through the protein-coding region (Fig. 2B). This change is likely to cause a loss of gene function since the C-terminal end of NHL-2 contains the NHL repeats, and these repeats are important for the RNA-binding function of many TRIM-NHL family proteins (Tocchini and Ciosk, 2015).

To support the conclusion that *sog-10(q162)* is allelic to *nhl-2*, we tested if the protein-null allele, *nhl-2(ok818)* (Hammell et al. 2009), phenocopied *sog-10(q162)* (Maine and Kimble, 1993). *nhl-2(ok818) glp-1(q224)* animals produce embryos at the restrictive temperature of 20 °C, confirming that the premature meiotic entry defect is suppressed (Table 1). We also observed an incompletely penetrant Fog phenotype in *nhl-2(ok818) XX* animals raised at 15 °C (Fig. 2C–E). We conclude that *sog-10(q162)* is a strong loss-of-function allele of *nhl-2*. We will refer to *q162* as an allele of *nhl-2* for the remainder of the paper.

3.2. NHL-2 is expressed throughout germ cell development

NHL-2 is a cytoplasmic protein ubiquitously expressed in most, if not all, cells throughout development (Hammell et al. 2009; Hyenne et al., 2008). Within cells, including the adult hermaphrodite germline and embryonic germ lineage, NHL-2 has been detected both as diffuse within the cytoplasm and in discrete cytoplasmic puncta (Hyenne et al. 2008; Davis et al. 2018) (Fig. 3). P granules are ribonucleoprotein (RNP) condensates and contain diverse RNA regulatory proteins, mRNAs, and small RNAs (sRNAs) and thought to be sites of extensive RNA regulation (Wang and Seydoux, 2013; Seydoux, 2018). We evaluated the distribution of NHL-2 in the developing germ line using immunolabeling. NHL-2 appeared mildly enriched in proliferating germ cells at all stages of larval development, with its level dropping modestly as germ cells entered meiotic prophase (Fig. 3A–F). NHL-2 was low or absent in germ cells that were visibly undergoing spermatogenesis (Fig. 3C). Consistent with published reports, we observed diffuse NHL-2 signal and small cytoplasmic puncta, including some that overlapped with perinuclear P granules (Fig. 3G).

3.3. NHL-2 inhibits germ stem cell fate and/or promotes meiotic entry

Since *nhl-2* mutations suppressed the premature meiotic entry phenotype of *glp-1(q224)* mutants, we predicted that *nhl-2* activity may normally inhibit the GSC fate and/or promote

meiotic entry. To explore further, we tested if loss of *nhl-2* function could enhance the tumorous phenotype of a weak *glp-1* gain-of-function (*gf*) allele, *ar202*. At 25 °C, *glp-1(ar202gf)* mutant gonads show a strong tumorous germline phenotype, and most germ cells fail to enter meiosis (Pepper et al. 2003). At semi-permissive temperatures of 15° and 20 °C, *glp-1(ar202gf)* mutant gonads show relatively mild extension of the progenitor zone compared to wildtype and otherwise retain a standard germline with meiotic nuclei and gametes (Hansen et al. 2004) (Fig. 4A). For this assay, we identified the progenitor zone by immunolabeling REC-8, a sister chromatid cohesion protein, under fixation conditions allowing its detection only in the nucleoplasm, and we identified meiotic nuclei by immunolabeling HIM-3, an axial component of the synaptonemal complex that associates with chromosomes in first meiotic prophase (Hansen et al. 2004). *glp-1(ar202gf)* mutants are sensitive to loss of gene products that inhibit the stem cell fate and/or promote meiotic entry (e.g., MacDonald et al. 2008; Chen and Greenwald, 2015; Safdar et al. 2016). We examined gonads from *nhl-2(ok818) glp-1(ar202gf)* double mutants and found that only a few germ cells had entered meiosis in 1-day old adults raised at 15 °C, and essentially no germ cells had entered meiosis in 1-day old adults raised at 20 °C (Fig. 4B). At 20 °C, 15/16 gonads scored contained no HIM-3 positive nuclei; all germline nuclei were REC-8 positive. 1/16 gonads had a very few HIM-3 positive nuclei; all other nuclei were REC-8 positive. This strong enhancement of the *glp-1(ar202gf)* tumorous phenotype is consistent with NHL-2 acting to inhibit the GSC fate and/or promote meiotic entry. To identify a more specific role for NHL-2, we examined the effect of *nhl-2(ok818)* on different components of the GSC gene regulatory network (Fig. 1), as described below.

3.4. LST-1 and SYGL-1 accumulation is unchanged in the *nhl-2(ok818)* background

GLP-1/Notch signaling induces *lst-1* and *sygl-1* transcription in the distal most ~5 cell diameters adjacent to the DTC, and LST-1 and SYGL-1 proteins together are required to prevent meiotic entry (Kershner et al. 2014; Lee et al. 2016; Haupt et al. 2020; Chen et al. 2020). Based on NHL-2 inhibiting the GSC fate, we asked whether NHL-2 might regulate expression of LST-1 and SYGL-1 accumulation within the distal end of the germ line. We evaluated LST-1::3xFLAG and 3xFLAG::SYGL-1 accumulation levels in *nhl-2(+)* controls and *nhl-2(ok818)* germlines. For each protein, the overall accumulation pattern was remarkably similar between *nhl-2(+)* and *nhl-2(ok818)*, except for a slight, although statistically significant, increase at two points in the peak levels for both LST-1 and SYGL-1 (Fig. 5). Importantly, there was no significant increase at proximal positions, indicating that the length of the stem cell pool in *nhl-2(ok818)* is the same as wildtype. Therefore, NHL-2 is unlikely to regulate LST-1 and/or SYGL-1 accumulation.

3.5. *nhl-2(ok818)* suppresses the premature meiotic entry phenotype of *fbf-1(0) fbf-2(0)*

We next examined the Pumilio-related genes, *fbf-1*, *fbf-2*, *puf-3* and *puf-11*, which function in conjunction with GLP-1 targets, *sygl-1* and *lst-1*, to repress the meiotic entry pathway genes (Fig. 1). At low culture temperatures (15°–20 °C), *fbf-1(0) fbf-2(0)* double mutants have a late-onset Glp-1-like phenotype where all GSCs prematurely enter meiosis during late larval development and form sperm (Crittenden et al. 2002) (Fig. 6A). Quadruple mutant animals, that also carry *puf-3(0)* and *puf-11(0)* mutations, have a stronger Glp-1-like null phenotype where all GSCs enter meiosis in early larval development, supporting

their redundant function in promoting the stem cell fate (Haupt et al. 2020). We tested whether *nhl-2(ok818)* could suppress the late-onset *fbf-1(0) fbf-2(0)* Glp-1-like phenotype by evaluating the germlines of *fbf-1(0) fbf-2(0); nhl-2(ok818)* triple mutant raised at low temperature. 100% of *fbf-1(0) fbf-2(0); nhl-2(ok818)* adult hermaphrodite germlines contained not only mature sperm, but also primary spermatocytes (indicating active spermatogenesis) and distal cells in meiotic prophase and/or mitotically cycling like cells (Fig. 6A). These results indicate that *nhl-2(ok818)* partially suppresses the *fbf-1(0) fbf-2(0)* premature meiotic entry defect in late larvae/early adults.

To further analyze the extent to which *nhl-2(ok818)* suppresses the *fbf-1(0) fbf-2(0)* genotype, we immunolabeled HIM-3. All *fbf-1(0) fbf-2(0); nhl-2(ok818)* germlines contained nuclei just distal to the primary spermatocytes where chromosome-associated HIM-3 was evident (n = 14), and most germlines contained progenitor zone-like nuclei without chromosome-associated HIM-3 at the distal end of the gonad arm (n = 13/14) (Fig. 6B). These results confirm that meiotic prophase nuclei are present in *fbf-1(0) fbf-2(0); nhl-2(ok818)* germlines at an age when they are no longer present in *fbf-1(0) fbf-2(0)* controls and, in addition, *fbf-1(0) fbf-2(0); nhl-2(ok818)* adults likely retain some GSCs. The suppression results are consistent with *nhl-2* opposing *fbf-1* and *fbf-2* activity, either directly or indirectly.

3.6. NHL-2 is a negative regulator of PUF-3 and PUF-11 accumulation in the distal germline

To examine whether PUF-3 and/or PUF-11 accumulation is altered in the *nhl-2(ok818)* mutant, we compared PUF expression in *nhl-2(ok818)* and *nhl-2(+)* germ lines. For these experiments, we assayed 3xV5::PUF-3 and 3xV5::PUF-11 produced from epitope-tagged endogenous alleles (Haupt et al. 2020) (see Methods). In wildtype adult hermaphrodites, PUF-3 and PUF-11 are present at relatively low levels in the progenitor zone and much higher levels in the proximal late meiotic prophase germ line (Haupt et al. 2020). We focused on the progenitor zone and quantified PUF expression across the distal 35 germ cell diameters (Fig. 7, Figs. S1 and S2). We observed a statistically significant increase in both PUF-3 and PUF-11 expression in the distal *nhl-2(ok818)* germ line compared to controls (Fig. 7A, Fig. S1). PUF-3 was significantly more abundant in *nhl-2(ok818)* compared to wildtype across the entire 35 distal germ cells, with the largest increase (~60%) at 5 cell diameters from the distal tip. In contrast, PUF-11 was significantly more abundant in *nhl-2(ok818)* compared to wildtype across the distal 13 germ cells and then dropped below wildtype level (Fig. 7A, Figs. S1 and S2). PUF-11 peaked more distally in *nhl-2(ok818)* (10–13 cell diameters) than in wildtype (19–21 cell diameters). At 5 cell diameters, PUF-11 was ~30% more abundant in *nhl-2(ok818)* than in wildtype. These results indicate that NHL-2 is a negative regulator of PUF-3 and PUF-11 accumulation in the progenitor zone. The increase in both PUF-3 and PUF-11 expression in *nhl-2(ok818)* provides an explanation, at least in part, for the suppression observed in the *fbf-1(0) fbf-2(0)* paralog double mutant, as well as the suppression of *glp-1(q224)* and the enhancement *glp-1(ar202gf)*.

3.7. NHL-2 does not appear to act in or downstream of the meiotic entry pathways

LST-1 and SYGL-1, together with FBF-1, FBF-2, PUF-3, and PUF-11, ensure the GSC fate by repressing the activity of three meiotic entry pathways mediated by GLD-1 (mutants have defective germline development), GLD-2, and SCF^{PROM-1} (ubiquitin ligase complex) (Fig. 1). These pathways repress translation of GSC factors, promote translation of meiotic factors, and promote turnover of progenitor zone proteins, respectively (Hubbard and Schedl, 2019). In single GLD-1, GLD-2, and SCF^{PROM-1} pathway mutants, meiotic entry occurs relatively normally. However, in animals carrying mutations in any two pathways, e.g., *gld-2(q497) gld-1(q485)* double mutants, meiotic entry is impaired, and a synthetic germline tumor develops (Kadyk and Kimble, 1998; Mohammad et al., 2018). One hypothesis for *nhl-2(ok818)* suppression of *glp-1(q224)* and *fbf-1(0) fbf-2(0)*, and the enhancement *glp-1(ar202gf)*, is that NHL-2 functions in or downstream of one or more of these meiotic entry pathways - perhaps in addition to its role in regulating PUF expression. We tested this idea by making double mutants carrying *nhl-2(ok818)* and a GLD-1 pathway mutant [*gld-1(q485)*, n = 30] or GLD-2 pathway mutant [*gld-2(q497)*, n = 27; *gld-3(q730)*, n = 22] and did not observe a synthetic tumor in any case. These results suggest that NHL-2 does not function in a meiotic entry pathway. To look more closely at a potential role for NHL-2 in meiotic entry, we used a sensitized genetic background where meiotic entry is weakly impaired. The synthetic germline tumor in *gld-2(q497); nos-3(oz231)* mutants is mild compared with *gld-2(q497) gld-1(q485)* mutants (Hansen et al. 2004; Mohammad et al., 2018). Adult *gld-2(q497); nos-3(oz231)* germlines have substantial numbers of meiotic nuclei whereas *gld-2(q497) gld-1(q485)* germlines have very few meiotic nuclei. We compared the synthetic tumor in *gld-2(q497); nos-3(oz231)* double mutants and *gld-2(q497); nos-3(oz231); nhl-2(ok818)* triple mutants (Fig. S3). We observed a similar distribution of REC-8 positive and HIM-3 positive nuclei in *gld-2(q497); nos-3(oz231)* [n = 16] and *gld-2(q497); nos-3(oz231); nhl-2(ok818)* [n = 15] gonad arms. Hence, *nhl-2(ok818)* did not obviously enhance the synthetic tumor. We interpret these results to indicate that NHL-2 likely does not act in or downstream of the GLD-1, GLD-2, or SCF^{PROM-1} meiotic entry pathway(s). Instead, NHL-2 may modulate progenitor zone size by acting solely upstream of these pathways.

3.8. NHL-2 promotes the normal size adult progenitor zone

In the *C. elegans* gonad, GLP-1/Notch signaling maintains germline stem cells, i.e., ensuring they do not differentiate, while nutritional and other inputs ensure robust mitotic proliferation of these cells (Singh and Hansen, 2017; Hubbard et al. 2013). During our studies, we noticed that *nhl-2* mutant adults had a smaller progenitor zone compared to *nhl-2(+)* controls based on marker protein analysis. In WAPL-1 staining experiments, the adult *nhl-2(ok818)* progenitor zone was shorter than in wildtype controls (17–18 vs 20 gcd) (Fig. 7; Fig. S2). Furthermore, the total number of cells in the *nhl-2(ok818)* progenitor zone was about 2/3 the number in wild type (Fig. S4), demonstrating a significant reduction in progenitor zone size. This *nhl-2* mutant phenotype seems counter to suppression of premature meiotic entry in *glp-1(q224)* partial loss of function and enhancement of the tumorous phenotype in *glp-1(ar202gf)*. Similarly, *puf-8(0)* is also an enhancer of *glp-1(ar202gf)* as well as promotes the normal size of the progenitor zone (see Introduction). The size of the progenitor zone is a complex interaction of multiple processes, including

the size of the stem cell pool, the rate of mitotic cell cycling, the rate of meiotic entry, and progenitor zone expansion during larval development, which is regulated by worm physiology (Hubbard and Schedl, 2019). Additional studies will be necessary to determine the basis of the smaller progenitor zone in *nhl-2* mutants, although the LST-1 and SYGL-1 immunolabeling data (Fig. 5) suggest that it is not an effect of the stem cell pool.

3.9. *nhl-2* RNAi phenotypes suggest germline specific NHL-2 functions

Because NHL-2 is widely expressed in most tissues throughout development, we wanted to determine if it acts specifically in germ cells to regulate germ cell processes. To address this question, we used a transgenic strain to RNAi knockdown *nhl-2* expression in germ cells and not in the somatic gonad (see Materials and Methods for details) (Fig. 8A–D). For simplicity, we refer to germline RNAi as *gRNAi*. In a *glp-1(ar202gf)* background, *nhl-2(gRNAi)* prevented most germ cells from entering meiosis compared to the *gfp(gRNAi)* control (Fig. 8A and B). We obtained consistent results when we performed *nhl-2* RNAi with *glp-1(oz264gf)*, another weak gain-of-function allele (Kerins et al., 2010), in the *rrf-1(0)* background where RNAi is disabled in the somatic gonad and many other somatic tissues (Kumsta and Hansen, 2012). In the *glp-1(oz264gf);rrf-1(0)* strain, *nhl-2* RNAi produced 94% (47/50) tumorous germlines, whereas *gfp* control RNAi produced 18% (7/38) tumorous germlines. We also observed the Fog phenotype in a subset of *nhl-2(gRNAi)* animals (Fig. 8E). Based on these results, NHL-2 activity is largely, if not exclusively, required in germ cells to influence the stem cell fate - meiotic development decision and to promote the male germ cell fate.

3.10. CGH-1 RNA helicase and ALG-5 Argonaute may participate with NHL-2 to inhibit the stem cell fate and/or promote meiotic entry

Genetic and biochemical data suggest that NHL-2 interacts with core components of the miRNA-induced silencing complex (miRISC) and with the conserved germline helicase, CGH-1, to facilitate microRNA-mediated repression of certain mRNAs in somatic tissues (Hammell et al. 2009; Alessi et al. 2015). CGH-1 is member of the conserved DDX6 family whose members are key components of RNA processing (P) bodies and participate in translational regulation and mRNA turnover in various organisms (reviewed by Rajyaguru and Parker, 2009). NHL-2 associates physically with CGH-1 as well as the miRNA Argonaute proteins, ALG-1 and ALG-2, in co-IP experiments and co-localizes with CGH-1 in protein-RNA condensates in germline and somatic tissues (Hammell et al. 2009; Davis et al. 2018). These findings prompted us to ask if NHL-2 might function together with CGH-1 or components of the core miRNA machinery in modulating the GSC fate vs meiotic entry decision. To examine this question, we first generated a *cgh-1(ok492) glp-1(ar202gf)* double mutant strain and evaluated the meiotic entry phenotype in adults at permissive temperature (20 °C) by immunostaining for REC-8 and HIM-3. As described above, *glp-1(ar202gf)* control germlines at 20 °C typically contain not only proliferative nuclei, but contain meiotic prophase nuclei as well. In contrast, for 5/48 *cgh-1(ok492) glp-1(ar202gf)* gonad arms, all germ cell nuclei were REC-8 positive and HIM-3 negative, indicating none had entered meiosis. Another 40/48 gonad arms included ectopic REC-8 positive nuclei intermixed with HIM-3 positive nuclei (Fig. 4C). Based on these data, the *glp-1(ar202gf)* weak tumorous phenotype was significantly enhanced in the *cgh-1(ok492) glp-1(ar202gf)* double mutant at

20 °C, consistent with CGH-1 acting to inhibit the stem cell fate and/or promote meiotic entry. Unfortunately, genetic experiments to evaluate if CGH-1 and NHL-2 act in a common pathway were not informative because (i) *cgh-1(ok492) nhl-2(ok818)* double mutants die at the L4 to adult molt [therefore we cannot test *cgh-1 nhl-2* for further suppression of *glp-1(q224)*], and (ii) the *nhl-2(ok818) glp-1(ar202gf)* tumorous phenotype was completely penetrant [therefore we cannot test for further enhancement by *cgh-1(RNAi)*].

Although no germline miRNAs have yet been identified as essential for the stem cell fate vs meiotic development decision (McEwen et al. 2016; Brown et al. 2017; Minogue et al. 2018; Dallaire et al. 2018; Theil et al. 2019), we decided to explore this possibility directly by testing if the *glp-1(ar202gf)* weak tumorous phenotype was enhanced by loss or knockdown of microRNA biogenesis factors or effector components of the pathway. We did not observe enhancement of *glp-1(ar202gf)* meiotic entry defects when knocking down or using mutant alleles of *alg-1*, *alg-2*, *dcr-1* (encoding Dicer endonuclease), *drsh-1* (encoding miRNA biogenesis factor, Drosha), or *pash-1* (encoding miRNA biogenesis factor, Pasha). Therefore, the core microRNA pathway may not act broadly to inhibit proliferative fate and/or promote meiotic entry.

In contrast to core miRNA pathway components, we observed strong enhancement of *glp-1(ar202gf)* when we knocked down *alg-5*. ALG-5 is the *C. elegans* Argonaute protein most closely related to ALG-1 and ALG-2, and it is expressed specifically in the germ line where it interacts with a subset of miRNAs and associates with P granules (Brown et al. 2017). We confirmed the *alg-5(RNAi)* result using *alg-5(tm1163)*, an in-frame deletion that removes much of the PAZ domain responsible for binding miRNA, and two nonsense mutations from the Million Mutant collection that are predicted to be null, *alg-5(gk119870)* and *alg-5(gk870731)*. All three alleles strongly enhanced the *glp-1(ar202gf)* phenotype. *alg-5(tm1163);nhl-2(ok818)* [n = 10] gonads contained almost entirely REC-8 positive germ cell nuclei with only a very few HIM-3 positive germ cell nuclei, as shown (Fig. 4D). Consistent with *glp-1(ar202gf)* enhancement, *alg-5(tm1163)* suppressed the *glp-1(q224)* loss-of-function phenotype in the germ line at 20 °C (Table 1). We conclude that ALG-5 promotes meiotic entry and/or inhibits the stem cell fate.

We further examined the relationship between NHL-2 and ALG-5 in promoting the stem cell fate in the *alg-5(tm1163);nhl-2(ok818) glp-1(q224)* triple mutant at 20 °C. Suppression of the *glp-1(q224)* germline phenotype in this triple mutant and the *nhl-2(ok818) glp-1(q224)* double mutant were similar (Table 1). This result is consistent with NHL-2 and ALG-5 acting in a common genetic pathway to promote meiotic entry and/or inhibit the stem cell fate.

4. Discussion

Here we identified *sog-10(q162)*, a mutation previously described as suppressing a germline GLP-1/Notch signaling defect (Maine and Kimble, 1993), as a strong loss-of-function allele of *nhl-2*. NHL-2 is a member of the broadly conserved TRIM-NHL family of proteins that includes other known cell fate regulators, including *Drosophila* Brat (Brain tumor) and MEI-P26 (meiotic P26), mammalian TRIM3 and TRIM32, and five *C. elegans* proteins

(Tocchini and Ciosk, 2015; Connacher and Goldstrohm, 2021). We identify several germline biological processes where NHL-2 functions, likely in an autonomous manner. NHL-2 is a negative regulator of the stem cell fate/positive regulator of meiotic entry, promotes the normal size of the progenitor zone, and has a minor role in promoting the male fate at lower culture temperatures.

Several lines of evidence support a role for NHL-2 in negatively regulating the stem cell fate. The loss of *nhl-2* function suppresses the premature meiotic entry phenotype of *glp-1(q224)* and enhances the weak tumorous phenotype of *glp-1(ar202gf)*. Downstream of GLP-1 signaling, four redundant Pumilio family RNA-binding proteins, FBF-1, FBF-2, PUF-3, and PUF-11, promote the stem cell fate (Haupt et al. 2020). We found that both PUF-3 and PUF-11 expression was increased in *nhl-2(ok818)* mutants, consistent with NHL-2 acting as a negative regulator of the stem cell fate. We also found that *nhl-2(ok818)* suppressed the premature meiotic entry phenotype of the *fbf-1(0) fbf-2(0)* double mutant. We speculate that the *fbf-1(0) fbf-2(0)* suppression is a result of increased PUF-3 and PUF-11 accumulation in the absence of *nhl-2*. Furthermore, we propose that suppression of *glp-1(q224)* and enhancement of *glp-1(ar202gf)* in *nhl-2(0)* are due to increased accumulation of the downstream PUF-3 and PUF-11 proteins (Fig. 9). NHL-2 acting at the level of PUF-3 and PUF-11 also explains why the embryonic lethal phenotype of *glp-1(q224)* was not suppressed, as the Pumilio proteins are not known to function downstream of GLP-1 signaling in the embryo. Based on the mutant phenotype, NHL-2 would appear to have a modulatory role as loss of the *nhl-2* gene on its own has relatively mild germline phenotypes. However, it remains possible that there is redundancy with other TRIM-NHL family members (see below).

Increased PUF-3 and PUF-11 accumulation could potentially result in feminization of the germline, providing an explanation for the *nhl-2(0)* incompletely penetrant Fog phenotype. FBF-1 and FBF-2 promote the female germ cell fate and are critical for the sperm-to-oocyte switch in the hermaphrodite, functioning to repress the expression of sex determination gene *fem-3* (Zhang et al. 1997). PUF-3 and PUF-11 could also function in repressing *fem-3*. However, we did not observe suppression of the *fbf-1(0) fbf-2(0)* masculinized germline following removal of *nhl-2* (Fig. 6) and the *puf-3(0) puf-11(0)* double mutant does not show obvious germline masculinization (Haupt et al. 2020). A possible explanation is that PUF-3 and PUF-11 have a minor contribution in promoting the female germ cell fate, relative to a major role for FBF-1 and FBF-2; this is consistent with the weak feminization by *nhl-2(0)*, and consistent with the smaller contribution of PUF-3 and PUF-11, relative to FBF-1 and FBF-2, in promoting the GSC fate (Haupt et al. 2020).

C. elegans TRIM-NHL proteins have numerous developmental functions, and our findings reinforce an emerging picture of TRIM-NHL proteins as context-dependent regulators. The *nhl-1*, *nhl-2*, *nhl-3*, and *ncl-1* genes were identified by genetic analysis to encode partially redundant regulators of asymmetric cell division in the embryo (Hyenne et al. 2008). Later work showed that NHL-2 positively regulates miRNA activity in the developing larva (Hammell et al. 2009; Karp and Ambros, 2012) and functions downstream of maternally provided miRNAs in the embryo to promote male development and viability (McJunkin and Ambros, 2017), which is distinct from its function in the male germ cell fate in XX

larval development described here. A fifth *C. elegans* TRIM-NHL protein, LIN-41, regulates developmental timing in the soma of larvae (Reinhart et al. 2000; Slack et al., 2000), and functions in oocyte meiotic maturation and the transition to embryogenesis (Spike et al. 2014b; Tocchini et al. 2014; Tsukamoto et al. 2017). The first report of a germline role for *nhl-2* was the finding of several defects in *nhl-2(ok818)* animals raised at moderate to high culture temperatures: abnormal meiotic chromosome segregation in developing oocytes, reduced brood size, a mortal germline (at 20°–25 °C), and embryonic lethality (at 23°–25 °C) (Davis et al., 2018). Their findings implicate NHL-2 activity as important for small interfering (si) RNA-mediated pathway functions in both germ line and soma. Our analysis of NHL-2 activity, carried out primarily at low-moderate temperatures (at 15°–20 °C) to take advantage of sensitized genetic backgrounds, complements this other work.

The temperature-sensitive consequences of reduced/absent NHL-2 activity, cold sensitivity (a feminized germline) and heat sensitivity (e.g., abnormal meiotic chromosome segregation), reveal processes that are temperature dependent, where NHL-2 functions to buffer this temperature dependence. We speculate that temperature-dependence may reflect different requirements for NHL-2 targets under different culture conditions, and/or temperature dependence of redundant factors. Significant differences in molecular phenotypes e.g., mRNA and small (s) RNA abundance, have been reported at 20° vs 25 °C (Davis et al. 2018). The effects of *nhl-2* loss on mRNA function and sRNA abundance at 20 °C may be particularly relevant to the GSC fate/meiotic development phenotypes that we observed. In contrast, gene expression changes relevant for the male germ cell fate in hermaphrodite larvae may only be detected at 15 °C.

TRIM-NHL proteins are known to function as RNA-binding proteins that regulate target mRNA activity and as E3 ubiquitin ligases to regulate protein turnover. As examples, mammalian TRIM32 promotes neuronal precursor differentiation by ubiquitinating cMyc (Hillje et al. 2011), and *C. elegans* LIN-41 promotes germline development by repressing translation of numerous target mRNAs (Spike et al. 2014a; Tocchini et al. 2014). Current data do not allow us to distinguish whether NHL-2 represses *puf-3* and *puf-11* expression at the level of translational repression/mRNA instability or protein turnover.

We identified two gene products, CGH-1 and ALG-5, that may act together with NHL-2 to influence the stem cell vs meiotic fate choice. Results supporting this possibility include that loss of each of the three genes enhances the tumorous phenotype of *glp-1(ar202gf)* and that loss of *nhl-2* or *alg-5* suppresses the premature meiotic entry phenotype of *glp-1(q224)* (*cgh-1* was not tested). Furthermore, NHL-2 physically associates with CGH-1, as well as miRNA Argonaute proteins ALG-1 and ALG-2, in co-IPs (Hammell et al. 2009; Davis et al. 2018) (ALG-5 was not tested). Our results do not support a role for core miRNA biogenesis factors in promoting the GSC fate/inhibiting meiotic development, as assayed by enhancement of *glp-1(ar202gf)*. In support of this negative result, *in situ* hybridization studies have failed to identify a germline expressed miRNA that accumulates in the progenitor zone (Minogue et al. 2018). Instead, NHL-2, ALG-5, and CGH-1 are positioned to interact with both siRNAs and PIWI-associated (pi) RNAs on P granules (Brown et al. 2017; Davis et al. 2018), and NHL-2 activity influences siRNA and piRNA abundance (Davis et al. 2018). Interestingly, the CSR-1 Argonaute complex, presumably through 22G

siRNAs, promotes the GSC fate/inhibits meiotic entry (Smardon et al. 2000; She et al. 2009). Possibly, NHL-2, ALG-5, and CGH-1 function to oppose the activity of the CSR-1 complex in this decision. Alternatively, or in addition, NHL-2 and CGH-1 may modulate the GSC versus meiotic fate choice in their capacity as translational regulators independent of small RNAs. CGH-1 localizes to numerous RNP particles in the *C. elegans* soma and germ line where translational regulation may occur (Navarro et al. 2001; Audhya et al. 2005; Boag et al. 2005; Jud et al. 2008; Noble et al. 2008), and it stabilizes certain maternal mRNAs (Noble et al. 2008; Boag et al., 2005) and represses expression of CED-3/caspase to limit apoptosis in the oogenic germ line (Subasic et al. 2016; Navarro et al. 2001).

In summary, we provide evidence that NHL-2 modulates the GSC fate vs meiotic development decision by inhibiting the accumulation of PUF-3 and PUF-11, likely explaining the genetic interactions observed with *nhl-2(0)*, suppression of the *glp-1(q224)* and *fbf-1(0) fbf-2(0)* GSC fate defects, and enhancement of *glp-1(ar202gf)* tumorous germline phenotype. An important future question is under what condition(s) does NHL-2 exert this modulatory activity, for example with age or nutrient status?

Supplementary Material

Refer to Web version on PubMed Central for supplementary material.

Acknowledgements

We thank: Li Qiao and Anne Smardon for fine structure genetic mapping of *q162*; Maria Ow, Niko Wagner, Matt Sullenberger, and Leanne Kelley for technical advice and assistance; Judith Kimble and Zuzana Kocisova for strains; Sarah Hall and members of the Schedl, Maine, and Hall labs for discussions; and Leanne Kelley and two anonymous reviewers for comments on the manuscript. Funding: This work was supported by the Syracuse University SOURCE program (to EMJ), the National Science Foundation (#IBN-9318709 to EMM), the National Institutes of Health (R01 GM100756 and GM63310 to TS), and Bio-MedRAP (to VJ). Some strains used in this study were provided by the Caenorhabditis Genetics Center, which is funded by NIH Office of Research Infrastructure Programs (P40 OD010440).

Data availability

Data will be made available on request.

References

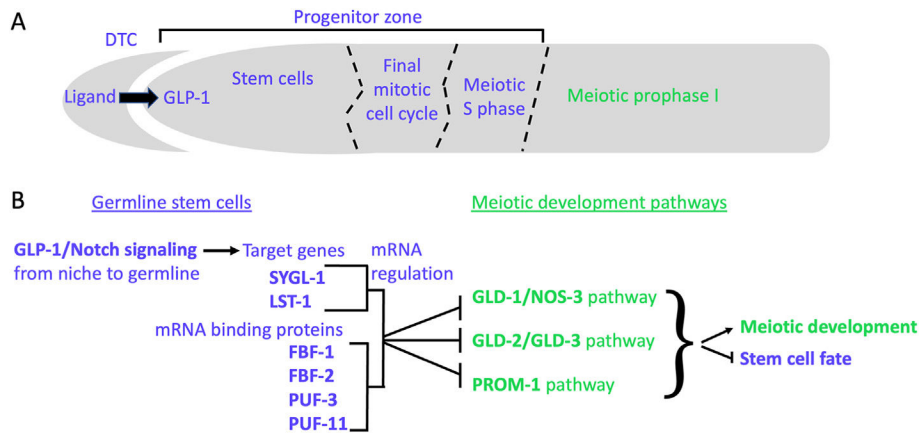
- Alessi AF, Khivansara V, Han T, Freeberg MA, Moresco JJ, Tu PG, Montoye E, Yates JR 3rd, Karp X, Kim JK, 2015. Casein kinase II promotes target silencing by miRISC through direct phosphorylation of the DEAD-box RNA helicase CGH-1. *Proc. Natl. Acad. Sci. USA* 112, E7213–E7222. 10.1073/pnas.1509499112. [PubMed: 26669440]
- Ariz M, Mainpal R, Subramaniam K, 2009. *C. elegans* RNA-binding proteins PUF-8 and MEX-3 function redundantly to promote germline stem cell mitosis. *Dev. Biol.* 326, 295–304. 10.1016/j.ydbio.2008.11.024. [PubMed: 19100255]
- Audhya A, Hyndman F, McLeod IX, Maddox AS, Yates JR 3rd, Desai A, Oegema K, 2005. A complex containing the Sm protein CAR-1 and the RNA helicase CGH-1 is required for embryonic cytokinesis in *Caenorhabditis elegans*. *J. Cell Biol.* 171, 267–279. 10.1083/jcb.200506124. [PubMed: 16247027]
- Austin J, Kimble J, 1987. *glp-1* is required in the germ line for regulation of the decision between mitosis and meiosis in *C. elegans*. *Cell* 51, 589–599. [PubMed: 3677168]

- Baudrimont A, Paouneskou D, Mohammad A, Lichtenberger R, Blundon J, Kim Y, Hartl M, Falk S, Schedl T, Jantsch V, 2022. Release of CHK-2 from PPM-1.D anchorage schedules meiotic entry. *Sci. Adv.* 8, eabl8861. 10.1126/sciadv.abl8861. [PubMed: 35171669]
- Boag PR, Nakamura A, Blackwell TK, 2005. A conserved RNA-protein complex component involved in physiological germline apoptosis regulation in *C. elegans*. *Development* 132, 4975–4986. 10.1242/dev.02060. [PubMed: 16221731]
- Brenner JL, Schedl T, 2016. Germline stem cell differentiation entails regional control of cell fate regulator GLD-1 in *Caenorhabditis elegans*. *Genetics* 202, 1085–1103. [PubMed: 26757772]
- Brown KC, Svendsen JM, Tucci RM, Montgomery BE, Montgomery TA, 2017. ALG-5 is a miRNA-associated Argonaute required for proper developmental timing in the *Caenorhabditis elegans* germline. *NAR* 45, 9093–9107. 10.1093/nar/gkx536. [PubMed: 28645154]
- Chen Y, Greenwald I, 2015. *hecd-1* modulates *Notch* activity in *Caenorhabditis elegans*. *G3 (Bethesda)* 5, 353–359. 10.1534/g3.114.015321.
- Chen J, Mohammad A, Pazdernik N, Huang H, Bowman B, Tycksen E, Schedl T, 2020. GLP-1 Notch-LAG-1 CSL control of the germline stem cell fate is mediated by transcriptional targets *Ist-1* and *sygl-1*. *PLoS Genet.* 10.1371/journal.pgen.1008650.
- Connacher RC, Goldstrohm AC, 2021. Molecular and Biological Functions of TRIM-NHL RNA Binding Proteins. *Wiley Interdiscip Review RNA.* 10.1002/wrna.1620.
- Crawley O, Barroso C, Testori S, Ferrandiz N, Silva N, Castellano-Pozo M, et al. , 2016. Cohesin-interacting protein WAPL-1 regulates meiotic chromosome structure and cohesion by antagonizing specific cohesion complexes. *Elife* 5, e10851. 10.7554/eLife.10851. [PubMed: 26841696]
- Crittenden SL, Bernstein DS, Bachorik JL, Thompson BE, Gallegos M, et al. , 2002. A conserved RNA-binding proteins controls germline stem cells in *Caenorhabditis elegans*. *Nature* 417, 660–663. 10.1038/nature754. [PubMed: 12050669]
- Crittenden SL, Leonhard KA, Burd DT, Kimble J, 2006. Cellular analyses of the mitotic region in the *Caenorhabditis elegans* adult germ line. *Mol. Biol. Cell* 17, 3051–3061. [PubMed: 16672375]
- Davis GM, Tu S, Anderson JW, Colson RN, Gunzburg MJ, Francisco MA, Ray D, Shrubsole SP, et al. , 2018. The TRIM-NHL protein NHL-2 is a co-factor in the nuclear and somatic RNAi pathways in *C. elegans*. *Elife* 7, e35478. 10.7554/eLife.35478. [PubMed: 30575518]
- Dallaire A, Frederick PM, Simard MJ, 2018. Somatic and germline microRNAs form distinct silencing complexes to regulate their target mRNAs differently. *Dev. Cell* 47, 239–247. 10.1016/j.devcel.2018.08.022 e4. [PubMed: 30245155]
- Fox PM, Schedl T, 2015. Analysis of germline stem cell differentiation following loss of GLP-1 Notch activity in *Caenorhabditis elegans*. *Genetics* 201, 167–184. [PubMed: 26158953]
- Fox PM, Vought VE, Hanazawa M, Lee M-H, Maine EM, Schedl T, 2011. Cyclin E and CDK-2 Regulate proliferative cell fate and cell cycle progression in the *C. elegans* germline. *Development* 138, 2223–2234. 10.1242/dev.059535. [PubMed: 21558371]
- Hammell CM, Lubin I, Boag PR, Blackwell TK, Ambros V, 2009. *nhl-2* modulates microRNA activity in *Caenorhabditis elegans*. *Cell* 136, 926–938. 10.1016/j.cell.2009.01.053. [PubMed: 19269369]
- Hansen D, Hubbard EJ, Schedl T, 2004. Multi-pathway control of the proliferation versus meiotic development decision in the *Caenorhabditis elegans* germline. *Dev. Biol.* 268, 342–357. 10.1016/j.ydbio.2003.12.023. [PubMed: 15063172]
- Haupt KA, Law KT, Enright AL, Kanzler CR, Shin H, Wickens M, Kimble J, 2020. A PUF hub drives self-renewal in *Caenorhabditis elegans* germline stem cells. *Genetics* 214, 147–161. 10.1534/genetics.119.302772. [PubMed: 31740451]
- Haupt KA, Enright AL, Ferdous AS, Kershner AM, Shin H, Wickens M, Kimble J, 2019. The molecular basis of LSR-1 self-renewal activity and its control of stem cell pool size. *Development* 146, dev181644. 10.1242/dev.181644. [PubMed: 31515205]
- Hillje AL, Worlitzer MM, Palm T, Schwamborn JC, 2011. Neural stem cells maintain their stemness through protein kinase C zeta-mediated inhibition of TRIM32. *Stem Cell.* 29, 1437–1447. 10.1002/stem.687.
- Hubbard EJA, Schedl T, 2019. Biology of the *Caenorhabditis elegans* germline stem cell system. *Genetics* 213, 1145–1188. 10.1534/genetics.119.300238. [PubMed: 31796552]

- Hubbard EJS, Korta DZ, Dalfo D, 2013. Physiological control of germline development. In: Germ Cell Development in *C. elegans*. T Schedl, Springer, New York, pp. 101–131. 10.1007/978-1-4614-4015-4_5.
- Hyenne V, Desrosiers M, Labbe JC, 2008. *C. elegans* Brat homologs regulate PAR protein-dependent polarity and asymmetric cell division. *Dev. Biol.* 321, 368–378. 10.1016/j.ydbio.2008.06.037. [PubMed: 18652816]
- Jaramillo-Lambert A, Ellefson M, Villeneuve AM, Engebrecht J, 2007. Differential timing of S phases, X chromosome replication, and meiotic prophase in the *C. elegans* germ line. *Dev. Biol.* 308, 206–221. [PubMed: 17599823]
- Jud MC, Czerwinski MJ, Wood MP, Young RA, Gallo CM, Bickel JS, Petty EL, Mason JM, Little BA, Padilla PA, Schisa JA, 2008. Large P body-like RNPs form in *C. elegans* oocytes in response to arrested ovulation, heat shock, osmotic stress, and anoxia and are regulated by the major sperm protein pathway. *Dev. Biol.* 318, 38–51. 10.1016/j.ydbio.2008.02.059. [PubMed: 18439994]
- Kadyk L, Kimble J, 1998. Genetic regulation of entry into meiosis in *Caenorhabditis elegans*. *Development* 125, 1803–1813. [PubMed: 9550713]
- Karp X, Ambros V, 2012. Dauer larva quiescence alters the circuitry of microRNA pathways regulating cell fate progression in *C. elegans*. *Development* 139, 2177–2186. 10.1242/dev.075986. [PubMed: 22619389]
- Kerins JA, Hanazawa M, Dorsett M, Schedl T, 2010. PRP-17 and the pre-mRNA splicing pathway are preferentially required for the proliferation versus meiotic development decision and germline sex determination in *Caenorhabditis elegans*. *Dev. Dynam.* 239, 1555–1572. 10.1002/dvdy.22274.
- Kershner AM, Shin H, Hansen TJ, Kimble J, 2014. Discovery of two GLP-1/Notch targets genes that account for the role of GLP-1/Notch signaling in stem cell maintenance. *Proc. Natl. Acad. Sci. USA* 111, 3739–3744. 10.1073/pnas.1401861111. [PubMed: 24567412]
- Kocsisova Z, Kornfeld K, Schedl T, 2019. Rapid population-wide declines in stem cell number and activity during reproductive aging in *C. elegans*. *Development* 146, dev173195. 10.1242/dev.173195. [PubMed: 30936182]
- Kosinski M, McDonald K, Schwartz J, Yamamoto I, Greenstein D, 2005. *C. elegans* sperm bud vesicles to deliver a meiotic maturation signal to distant oocytes. *Development* 132, 3357–3369. [PubMed: 15975936]
- Kumsta C, Hansen M, 2012. *C. elegans rrf-1* mutations maintain RNAi efficiency in the soma in addition to the germline. *PLoS One* 7, e35428. 10.1371/journal.pone.0035428. [PubMed: 22574120]
- Lee C, Sorensen EB, Lynch TR, Kimble J, 2016. *C. elegans* GLP-1/Notch activates transcription in a probability gradient across the germline stem cell pool. *Elife* 5, e18370. 10.7554/eLife.18370. [PubMed: 27705743]
- MacDonald LD, Knox A, Hansen D, 2008. Proteasomal regulation of the proliferation vs meiotic entry decision in the *Caenorhabditis elegans* germ line. *Genetics* 180, 905–920. 10.1534/genetics.108.091553. [PubMed: 18791239]
- Maciejowski J, Ugel N, Mishra B, Isopi M, Hubbard EJ, 2006. Quantitative analysis of germline mitosis in adult *C. elegans*. *Dev. Biol.* 292, 142–151. [PubMed: 16480707]
- Maine EM, Kimble J, 1993. Suppressors of *glp-1*, a gene required for cell communication during development in *Caenorhabditis elegans*, define a set of interacting genes. *Genetics* 135, 1011–1022. 10.1093/genetics/135.4.1011. [PubMed: 8307319]
- Marré J, Traver EC, Jose AM, 2016. Extracellular RNA is transported from one generation to the next in *Caenorhabditis elegans*. *Proc. Natl. Acad. Sci. U. S. A.* 113, 12496–12501. 10.1073/pnas.1608959113. [PubMed: 27791108]
- McEwen TJ, Yao Q, Yun S, Lee CY, Bennett KL, 2016. Small RNA in situ hybridization in *Caenorhabditis elegans*, combined with RNA-seq, identifies germline-enriched microRNAs. *Dev. Biol.* 418, 248–257. 10.1016/j.ydbio.2016.08.003. [PubMed: 27521456]
- McJunkin K, Ambros V, 2017. A microRNA family exerts maternal control on sex determination in *C. elegans*. *Genes Dev.* 31, 422–437. 10.1101/gad.290155.116. [PubMed: 28279983]

- Michaelson D, Korta DZ, Capua Y, Hubbard EJ, 2010. Insulin signaling promotes germline proliferation in *C. elegans*. *Development* 137, 671–680. 10.1242/dev.042523. [PubMed: 20110332]
- Minogue AL, Tacjett MR, Atabakhsh E, Tejada G, Arur S, 2018. Functional genomic analysis identifies miRNA repertoire regulating *C. elegans* oocyte development. *Nat. Commun.* 9, 5318. 10.1038/s41467-018-07791-w. [PubMed: 30552320]
- Mohammad A, Vanden Broek K, Wang C, Daryabeigi A, Jantsch V, et al. , 2018. Initiation of meiotic development is controlled by three post-transcriptional pathways in *Caenorhabditis elegans*. *Genetics* 209, 1197–1224. 10.1534/genetics.118.300985. [PubMed: 29941619]
- Navarro RE, Shim EY, Kohara Y, Singson A, Blackwell TK, 2001. *cgh-1*, a conserved predicted RNA helicase required for gametogenesis and protection from physiological germline apoptosis in *C. elegans*. *Development* 128, 3221–3232. 10.1242/dev.128.17.3221. [PubMed: 11546739]
- Noble SL, Allen BL, Goh LK, Nordick K, Evans TC, 2008. Maternal mRNAs are regulated by diverse P body-related mRNP granules during early *Caenorhabditis elegans* development. *J. Cell Biol.* 182, 559–572. 10.1083/jcb.200802128. [PubMed: 18695046]
- Pepper AS, Killian DJ, Hubbard EJ, 2003. Genetic analysis of *Caenorhabditis elegans glp-1* mutants suggests receptor interaction or competition. *Genetics* 163, 115–132. 10.1093/genetics/163.1.115. [PubMed: 12586701]
- Racher H, Hansen D, 2012. PUF-8, a Pumilio homolog, inhibits the proliferative fate in *Caenorhabditis elegans* germline. *G3 (Bethesda)* 2, 1197–1205. 10.1534/g3.112.003350. [PubMed: 23050230]
- Rajyaguru P, Parker R, 2009. CGH-1 and the control of maternal mRNAs. *Trends Cell Biol.* 19, 24–28. 10.1016/j.tcb.2008.11.001. [PubMed: 19062290]
- Rastogi S, Borgo B, Pazdernik N, Fox P, Mardis ER, Kohara Y, Havranek J, Schedl T, 2015. *Caenorhabditis elegans glp-4* encodes a valyl aminoacyl tRNA synthetase. *G3 (Bethesda)* 5, 2719–2728. 10.1534/g3.115.021899. [PubMed: 26464357]
- Reinhart BJ, Slack FJ, Basson M, Pasquinelli AE, Bettinger JC, Rougvie AE, Horvitz HR, Ruvkun G, 2000. *Nature* 403, 901–906. 10.1038/35002607. [PubMed: 10706289]
- Safdar K, Gu A, Xu X, Au V, Taylor J, Flibotte S, Moerman DG, Maine EM, 2016. UBR-5, a conserved HECT-type E3 ubiquitin ligase, negatively regulates Notch-type signaling in *C. elegans*. *G3 (Bethesda)* 6, 2125–2134. 10.1534/g3.116.027805. [PubMed: 27185398]
- Seidel HC, Kimble J, 2015. Cell-cycle quiescence maintains *Caenorhabditis elegans* germline stem cells independent of GLP-1/Notch. *Elife* 4, e10832. 10.7554/eLife.10832. [PubMed: 26551561]
- Seydoux G, 2018. The P granules of *C. elegans*: a genetic model for the study of RNA-protein condensates. *J. Mol. Biol.* 430, 4702–4710. 10.1016/j.jmb.2018.08.007. [PubMed: 30096346]
- She X, Xu X, Fedotov A, Kelly WG, Maine EM, 2009. Regulation of heterochromatin assembly on unpaired chromosomes during *Caenorhabditis elegans* meiosis by components of a small RNA-mediated pathway. *PLoS Genet.* 5, e1000624. 10.1371/journal.pgen.1000624. [PubMed: 19714217]
- Shin H, Haupt KA, Kershner AM, Kroll-Conner P, Wickens M, Kimble J, 2017. SYGL-1 and LST-1 link niche signaling to PUF RNA repression for stem cell maintenance in *Caenorhabditis elegans*. *PLoS Genet.* 13, e1007121. 10.1371/journal.pgen.1007121. [PubMed: 29232700]
- Singh R, Hansen D, 2017. Regulation of the balance between proliferation and differentiation in germ line stem cells. *Results Probl. Cell Differ.* 59, 31–66. 10.1007/978-3-319-44820-6_2.
- Slack FJ, Basson M, Liu Z, Ambros V, Horvitz HR, Ruvkun G, 2000. The *lin-41* RBCC gene acts in the *C. elegans* heterochronic pathway between the *let-7* regulatory RNA and the LIN-29 transcription factor. *Mol. Cell.* 5, 659–669. 10.1016/s1097-2765(00)80245-2. [PubMed: 10882102]
- Smardon A, Spoerke JM, Stacey SC, Klein ME, Mackin N, Maine EM, 2000. EGO-1 is related to RNA-directed RNA polymerase and functions in germ-line development and RNA interference in *C. elegans*. *Curr. Biol.* 10, 169–178. 10.1016/s0960-9822(00)00323-7. [PubMed: 10704412]
- Spike CA, Coetzee D, Eichten C, Wang X, Hansen D, Greenstein D, 2014a. The TRIM-NHL protein LIN-41 and OMA RNA-binding proteins antagonistically control the prophase-to-metaphase transition and growth of *Caenorhabditis elegans* oocytes. *Genetics* 198, 1535–1558. 10.1534/genetics.114.168831. [PubMed: 25261698]

- Spike CA, Coetzee D, Nishi Y, Guven-Ozkan T, Oldenbroek M, Yamamoto I, Lin R, Greenstein D, 2014b. Translational control of the oogenic program by components of OMA ribonucleoprotein particles in *Caenorhabditis elegans*. *Genetics* 198, 1513–1533. 10.1534/genetics.114.168823. [PubMed: 25261697]
- Subasic D, Stoeger T, Eisenring S, Matia-Gonzalez AM, Imig J, Zheng X, Xiong L, et al. , 2016. Post-transcriptional control of executioner caspases by RNA-binding proteins. *Genes Dev.* 30, 2213–2225. 10.1101/gad.285726.116. [PubMed: 27798844]
- Theil K, Imami K, Rajewsky N, 2019. Identification of proteins and miRNAs that specifically bind an mRNA in vivo. *Nat. Commun.* 10, 4205. 10.1038/s41467-019-12050-7. [PubMed: 31527589]
- Timmons L, Court DL, Fire A, 2001. Ingestion of bacterially expressed dsRNAs can produce specific and potent genetic interference in *Caenorhabditis elegans*. *Gene* 263, 103–112. 10.1016/S0378-1119(00)00579-5. [PubMed: 11223248]
- Tocchini C, Ciosk R, 2015. TRIM-NHL proteins in development and disease. *Semin. Cell Dev. Biol.* 47–48, 52–59. 10.1016/j.semcdb.2015.10.017.
- Tocchini C, Keusch JJ, Miller SB, Finger S, Gut H, Stadler MB, Ciosk R, 2014. The TRIM-NHL protein LIN-41 controls the onset of developmental plasticity in *Caenorhabditis elegans*. *PLoS Genet.* 10, e1004533. 10.1371/journal.pgen.1004533. [PubMed: 25167051]
- Tsukamoto T, Gearhart MD, Spike CA, Huelgas-Morales G, Mews M, Boag PR, Beilharz TH, Greenstein D, 2017. LIN-41 and OMA ribonucleoprotein complexes mediate a translational repression-to-activation switch controlling oocyte meiotic maturation and the oocyte-to-embryo transition in *Caenorhabditis elegans*. *Genetics* 206, 2007–2039. 10.1534/genetics.117.203174. [PubMed: 28576864]
- Wang JT, Seydoux G, 2013. Germ cell specification. *Adv. Exp. Med. Biol.* 757, 17–39. 10.1007/978-1-4614-4015-4_2. [PubMed: 22872473]
- Zhang B, Gallego M, Pouti A, Durkin E, Fields S, Kimble J, Wickens MP, 1997. A conserved RNA-binding protein that regulates sexual fates in the *C. elegans* hermaphrodite germ line. *Nature* 390, 477–484. 10.1038/37297. [PubMed: 9393998]

**Fig. 1.**

Genetic regulatory network controlling the germline stem cell fate versus meiotic development decision. (A) Illustration shows the relative positions of the distal tip cell (DTC), cells in the progenitor zone, and cells in early meiotic prophase I. (B) Diagrammatic representation of key regulatory factors for the germline stem cell fate versus meiotic entry decision in the *C. elegans* germ line. Ligand is expressed in the DTC, and GLP-1/Notch receptor is expressed in the germ line. GLP-1/Notch signaling from the DTC niche to germ cells upregulates transcription of the stem cell regulators, *lst-1* and *sygl-1*, whose protein products interact with components of the PUF hub (FBF-1, FBF-2, PUF-3, PUF-11). LST-1/PUF and SYGL-1/PUF complexes are thought to act, at least in part, in translational repression of *gld-1* and *gld-2* mRNA (Haupt et al. 2019, 2020). As germ cells move proximally, exiting the niche, concentrations of SYGL-1 and LST-1 self-renewal factors decrease, and the meiotic entry pathways become active. We note that PUF-8 is not included in the illustration because its position relative to the pathway is not known.

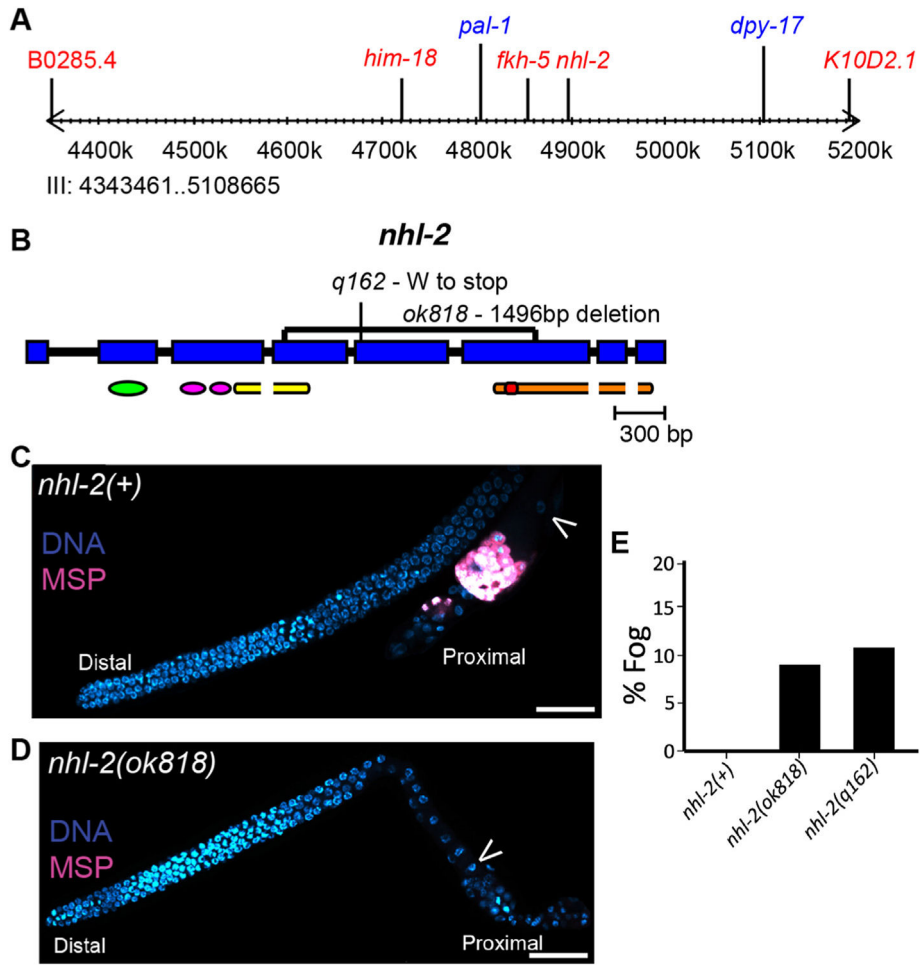


Fig. 2. *sog-10(q162)* is allelic to *nhl-2*.

(A) Summary of three-factor mapping and whole genome sequencing data used to identify *q162*. Mapping suggested *q162* was located between *pal-1* and *dpy-17* (blue text). Whole genome sequencing identified two protein-coding mutations within this region and three others in nearby flanking regions (red text). RNAi of each of these five genes was tested for suppression of *glp-1(q224)* fertility defects (see text). Genomic map was obtained from www.wormbase.org version WS251 genome browser and modified in Adobe Illustrator to highlight positions of genes identified with coding mutations and the positions of *pal-1* and *dpy-17*. (B) *nhl-2* gene model. Blue boxes represent exons, intersecting lines represent introns. Relative positions of conserved domains are indicated below: a RING domain (green), a ZnF/B-Box (magenta), a C-terminal B-Box (yellow), and several NHL-repeats (orange, with a single NHL repeat in red to show scale). *q162* is a nonsense mutation at amino acid residue 484 (tryptophan). The *ok818* deleted region is indicated with a bracket. (C) Representative image of wildtype hermaphrodite gonad at young adult stage, ~4 h post-L4 molt, at 15 °C. Spermatids are present in the proximal gonad arm and contain major sperm proteins (MSP) as detected by immunolabeling. (D) Representative image of a *nhl-2(ok818)* hermaphrodite gonad ~4 h post-L4 molt at 15 °C displaying a feminized germline (Fog) phenotype. No spermatids or spermatocytes are observed and thus no MSP-positive cells are present. Arrowhead in C and D indicates the position of the most proximal

oocyte nucleus. Scale bars, 25 μm . (E) Bar graph showing percentage of gonads scored that are MSP negative and thus Fog at 15 °C.

Author Manuscript

Author Manuscript

Author Manuscript

Author Manuscript

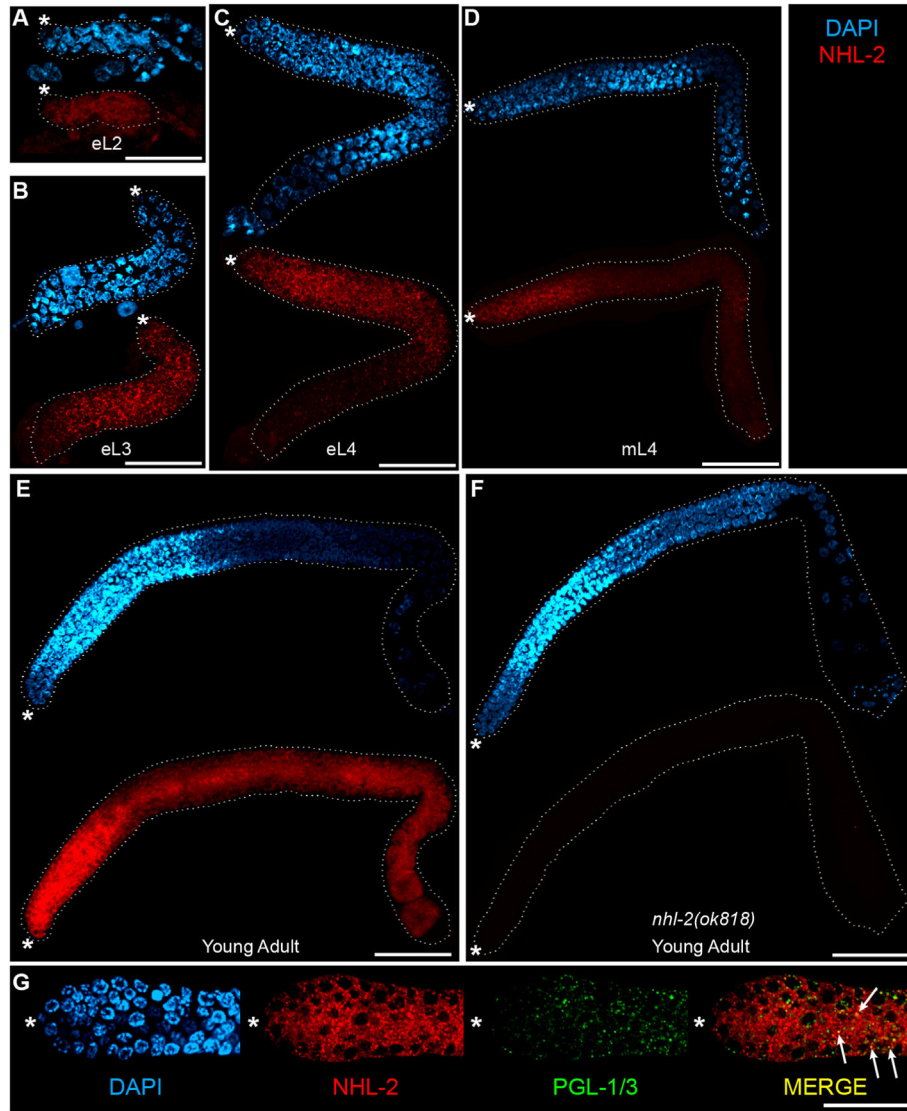


Fig. 3. NHL-2 is expressed throughout germline development.

Dissected gonads were stained with DAPI to visualize DNA (blue-cyan, top) and immunolabeled with anti-NHL-2 (bottom, red). *, distal end of the gonad arm. Images show the wildtype gonad at multiple stages of development: (A) early L2 larval stage (eL2), (B) early L3 larval stage (eL3), (C) early L4 stage (eL4), (D) mid L4 stage (mL4), (E) young adult stage ~12 h past L4. (F) Young adult gonad from an *nhl-2(ok818)* protein null mutant. NHL-2 labeling was largely absent; weak, punctate label was visible in the nucleolus, which might reflect cross-reaction of antibodies to paralogous proteins NCL-1 or NHL-3. (G) Higher magnification view of the distal wildtype gonad immunolabeled with anti-NHL-2 and anti-PGL-1/3. PGL-1 and PGL-3 are constitutive P granules components. Some P granules co-labeled with NHL-2 are visible in the merged image, consistent with published reports that NHL-2 associates with P granules. Numerous NHL-2 puncta dispersed throughout the cytoplasm do not co-label with PGL-1/3 and appear to be distinct from P granules. Scale bar, 25 μ m.

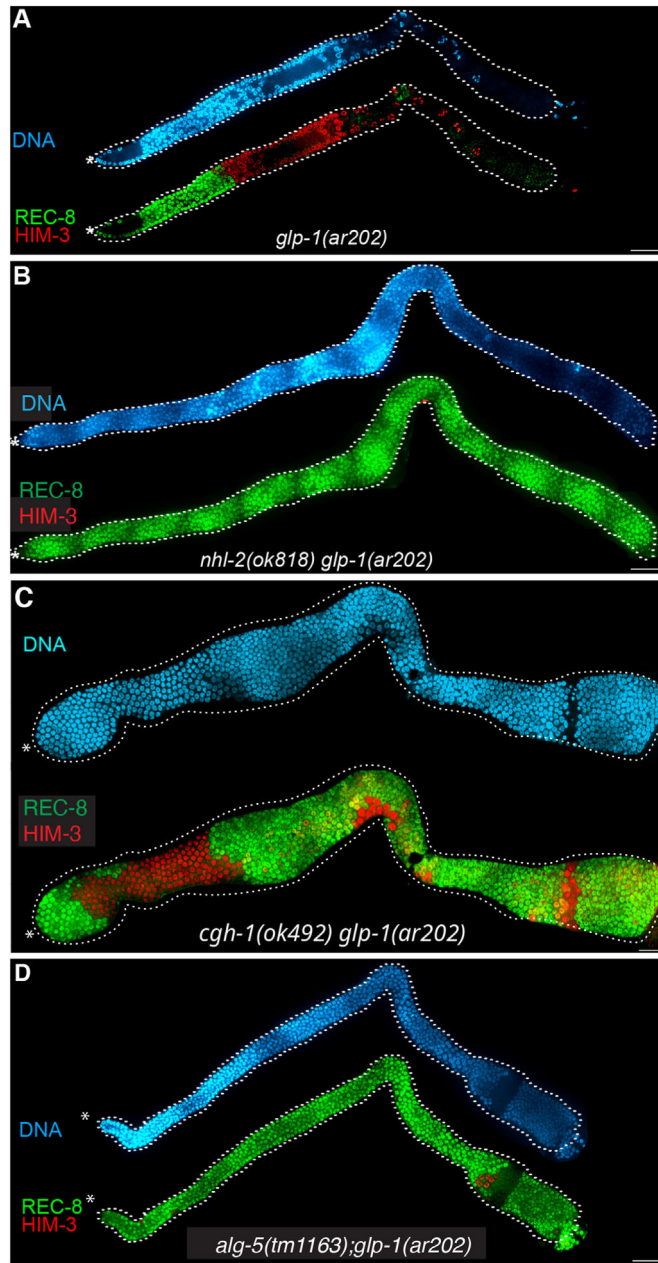


Fig. 4. Loss of NHL-2 function enhances the weak *glp-1(gf)* tumorous phenotype.

Images show dissected gonads from 1-day old adult hermaphrodites raised at 20 °C that are stained with DAPI to visualize DNA (top) and immunolabeled with anti-REC-8 (green, bottom) and anti-HIM-3 (red, bottom) antibodies. *, distal end of the gonad arm; gonads are outlined with a dotted line. (A) Representative *glp-1(ar202gf)* gonad at 20 °C. Progenitor zone nuclei have prominent REC-8 label, and meiotic prophase nuclei have prominent HIM-3 signal. (B) Representative *nhl-2(ok818) glp-1(ar202gf)* gonad contains a germline tumor with essentially no meiotic nuclei. (C) Representative *cgh-1(ok492) glp-1(ar202gf)* gonad containing ectopic REC-8 positive (progenitor) nuclei intermixed with patches of

HIM-3 positive (meiotic) nuclei. (D) Representative *alg-5(tm1163); glp-1(ar202gf)* gonad is filled progenitor nuclei and contains a very few meiotic nuclei. Scale bars, 50 μm .

Author Manuscript

Author Manuscript

Author Manuscript

Author Manuscript

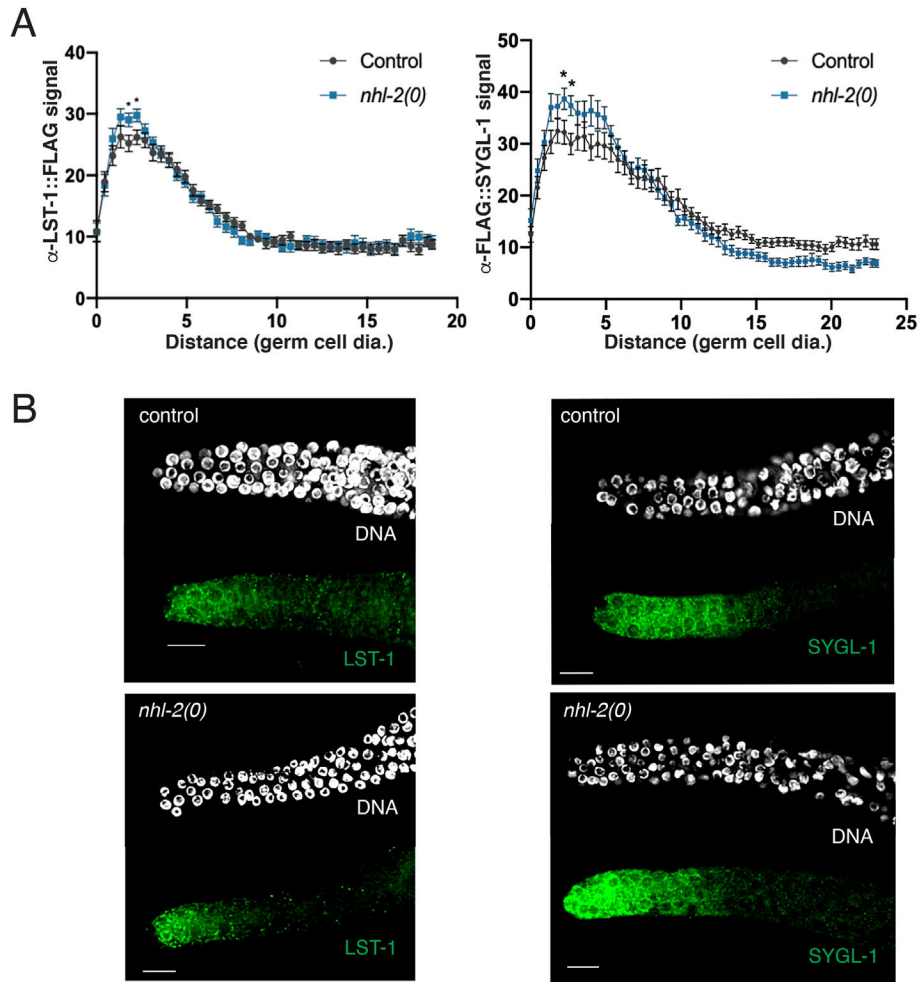


Fig. 5. LST-1 and SYGL-1 are upregulated in the *nhl-2(ok818)* background.

(A) Adults carrying *LST-1::3xFLAG* (left) or *3xFLAG::SYGL-1* (right) were immunolabeled with anti-FLAG antibody at 24 h post-L4 stage and stained with DAPI to visualize DNA. Control indicates *nhl-2(+)*, and *nhl-2(0)* indicates *nhl-2(ok818)*. Protein level (Y-axis) from immunolabeling is plotted in arbitrary units (mean grey value; see Methods); baseline has a value of ~10. Distance from the distal tip of the gonad (X-axis) is plotted in germ cell diameters. Genotypes and sample size: *3xflag::lst-1* [n = 19], *3xflag::lst-1; nhl-2(0)* [n = 20], *3xflag::sygl-1* [n = 34] and *3xflag::sygl-1; nhl-2(0)* [n = 23] gonad arms. The LST-1 and SYGL-1 accumulation patterns are remarkably similar between wild type and *nhl-2(0)*, particularly at proximal positions that determine size of the stem cell pool, except for a slight, but significant, higher peak level in *nhl-2(0)* than in wildtype, *p < 0.05. (B) Examples of LST-1 and SYGL-1 immunolabeling in *nhl-2(+)* control and *nhl-2(ok818)* distal germ lines. Distal gonad end is to the left, consistent with graphs in (A). Scale bars, 10 μ m.

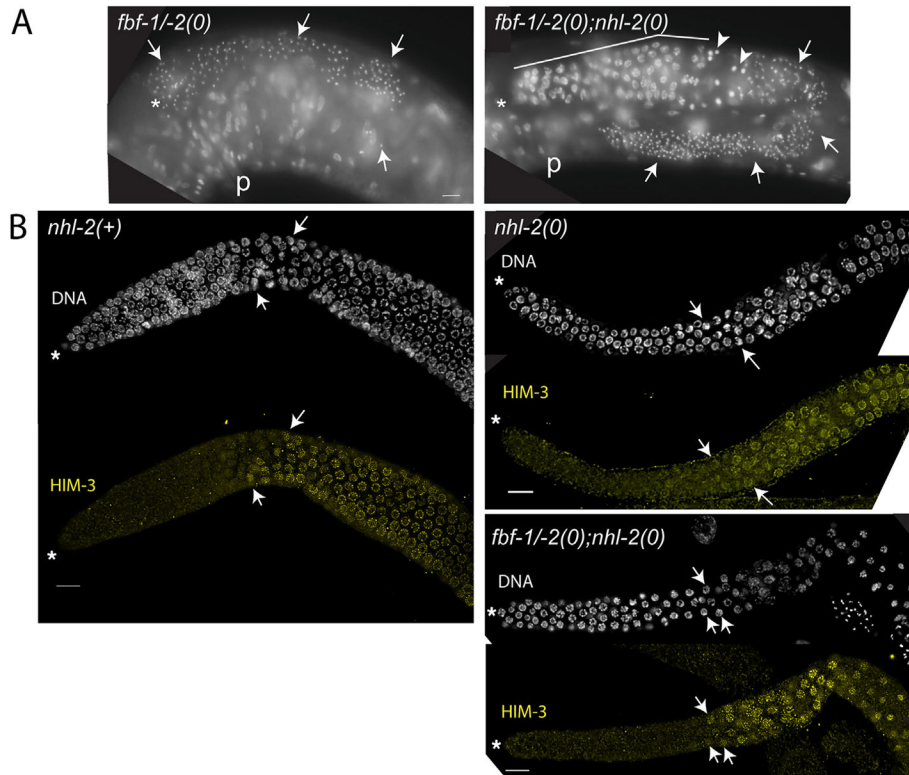


Fig. 6. Loss of NHL-2 suppresses the *fbf-1 fbf-2* premature meiotic entry defect.

(A) Intact adult hermaphrodites were fixed at 24 h post-L4 stage and DAPI-stained to visualize DNA. One representative gonad arm is shown. *, distal end of the gonad arm; p, proximal gonad. In the image labels, *fbf-1/-2(0)* indicates *fbf-1(0) fbf-2(0)*, and *nhl-2(0)* indicates *nhl-2(ok818)*. Left, *fbf-1(0) fbf-2(0)* germlines contain only mature sperm (arrows), whereas right, *fbf-1(0) fbf-2(0); nhl-2(ok818)* germlines include mature sperm (arrows), primary spermatocytes (arrowheads), and additional, progenitor zone-like distal germ cells (bar). We note that *fbf-1(0) fbf-2(0); nhl-2(ok818)* triple mutants were Mog (see text). *fbf-1(0) fbf-2(0)* [n = 36] and *fbf-1(0) fbf-2(0); nhl-2(ok818)* [n = 58]. (B) Representative images of dissected adult hermaphrodite gonads stained with DAPI (upper) and labeled with anti-HIM-3 (lower, gold) at 24 h post-L4 stage. *, distal end of the gonad arm. Images are maximum projections of Z-stacks processed by deconvolution (see Methods). Arrows indicate the distal most nuclei containing labeled HIM-3, and the corresponding DAPI stained nuclei. *nhl-2(+)* and *nhl-2(ok818)* germlines contained a distal progenitor zone where HIM-3 was not detected on chromosomes, as expected; nuclei located proximal to this region contain chromosome-associated HIM-3, consistent with first meiotic prophase. In *fbf-1/2(0); nhl-2(ok818)* germlines, HIM-3 was detected on chromosomes in nuclei distal to the primary spermatocytes, indicating they are in first meiotic prophase. Most germlines also contained progenitor zone-like nuclei at the distal end of the gonad arm where HIM-3 chromosomal staining was not observed. We note that occasionally *nhl-2(ok818)* controls and *fbf-1(0) fbf-2(0); nhl-2(ok818)* triple mutants had one or a few nuclei with chromosome-associated HIM-3 within the progenitor zone and/or without chromosome-associated HIM-3 within the pachytene zone. Scale bars, 10 μm.

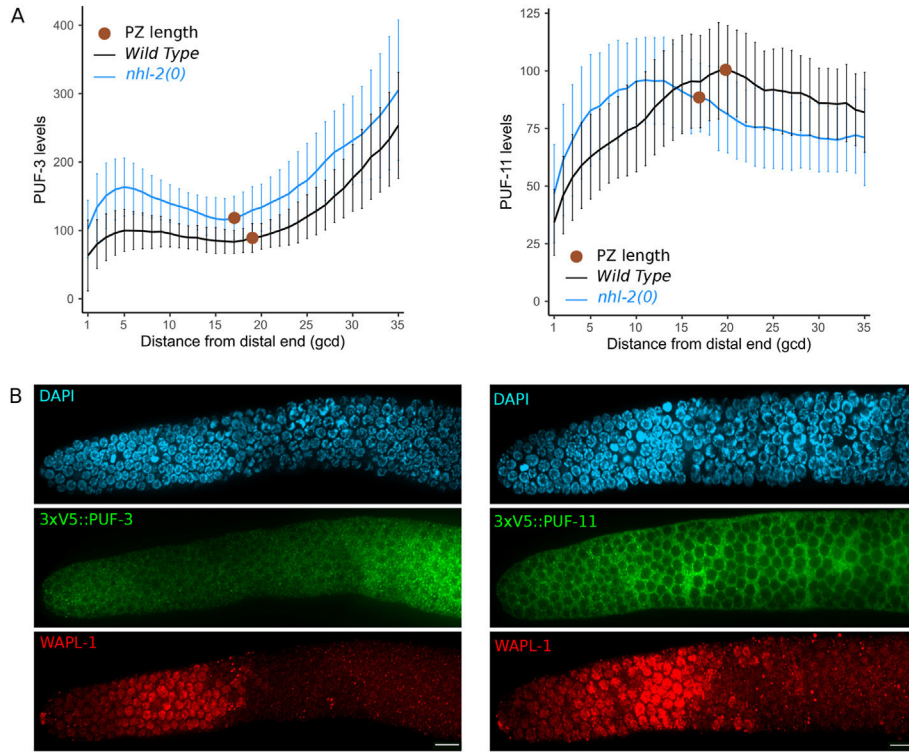


Fig. 7. PUF-3 and PUF-11 levels are elevated in the distal *nhl-2(ok818)* germ line.

(A) Line plots show 3xV5::PUF-3 or 3xV5::PUF-11 protein levels in wildtype and *nhl-2(ok818)* mutants [designated *nhl-2(0)*]. Protein levels were measured over 35 germ cell diameters (gcd) from the distal end; red dot indicates the proximal boundary of the progenitor zone as defined by WAPL-1 staining, a cohesion-removal protein that is down-regulated at meiotic entry (Crawley et al. 2016). Protein levels are shown in arbitrary units; a value of 100 units was set for each protein at the position within the first 20 cell diameters with the strongest wildtype signal. This position is at 5 cell diameters for 3xV5::PUF-3 and 20 cell diameters for 3xV5::PUF-11. Error bars indicate ± 1 SD. PUF-3 abundance was significantly higher in *nhl-2(ok818)* than *nhl-2(+)* across the entire region assayed. PUF-11 abundance was significantly higher in *nhl-2(ok818)* than in *nhl-2(+)* across the region except for several points at/near where the two lines cross. Statistical significance at each data point is indicated in a dotplot in Fig. S1. Genotype and sample size: left, *nhl-2(+)*; 3xV5::*puf-3* [n = 82], *nhl-2(0)*; 3xV5::*puf-3* [n = 93], right, *nhl-2(+)*; 3xV5::*puf-11* [n = 83], *nhl-2(0)*; 3xV5::*puf-11* [n = 90]. (See Materials and Methods.) (B) Images show the distal portions of adult wildtype gonads labeled with anti-V5 antibody to visualize 3xV5::PUF-3 (left) or 3xV5::PUF-11 (right), anti-WAPL-1, and DAPI, as indicated. Distal gonad end is to the left, consistent with (A). Fig. S2 shows an example of 3xV5::PUF-11 labeling in *nhl-2(ok818)*. Scale bars, 10 μ m.

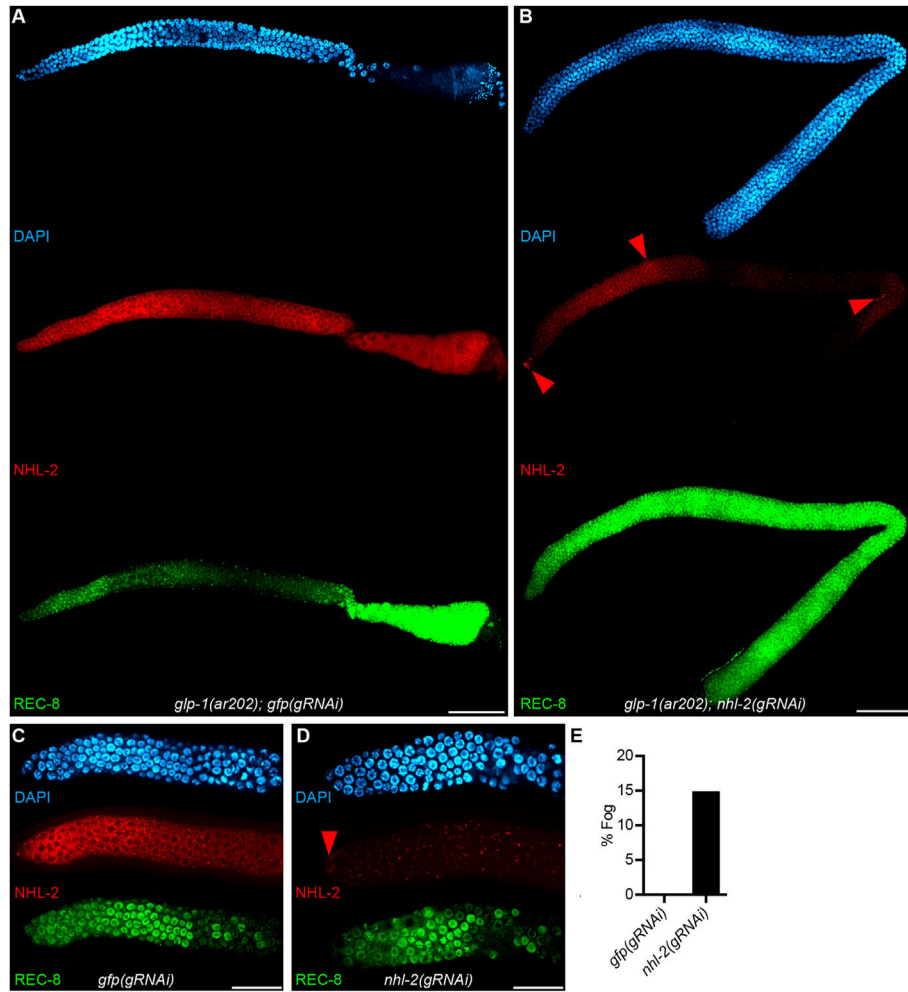


Fig. 8. Germ cell-specific RNAi phenocopies germ cell phenotypes of *nhl-2(null)* mutants. “*gRNAi*” indicates germline RNAi, as described in the text. (A) Representative control *glp-1(ar202); gfp(gRNAi)* gonad stained with DAPI to visualize DNA (cyan; top) and immunolabeled with anti-NHL-2 (red; middle) and anti-REC-8 (green, bottom). REC-8 signal decreases as germ cells enter meiosis then increases during oogenesis. (B) Representative *glp-1(ar202); nhl-2(gRNAi)* gonad labeled as in (A). REC-8 remains elevated in all germ cell nuclei with no obvious entry into meiosis despite incomplete knockdown of NHL-2 in the distal gonad. (C) Distal end of a representative control *gfp(gRNAi)* gonad and (D) representative *nhl-2(gRNAi)* gonad labeled as in (A). NHL-2 is depleted in these germ cells. Red triangles in B and D point to somatic cells of the gonad where NHL-2 levels remain high. (E) Percent of gonads without visible spermatids or primary spermatocytes (% Fog) for control *gfp(gRNAi)* versus *nhl-2(gRNAi)* gonads (n = 105). Distal end of each gonad arm is to the left. Scale bars are 50 μ m in A and B, 25 μ m in C, and 20 μ m in D.

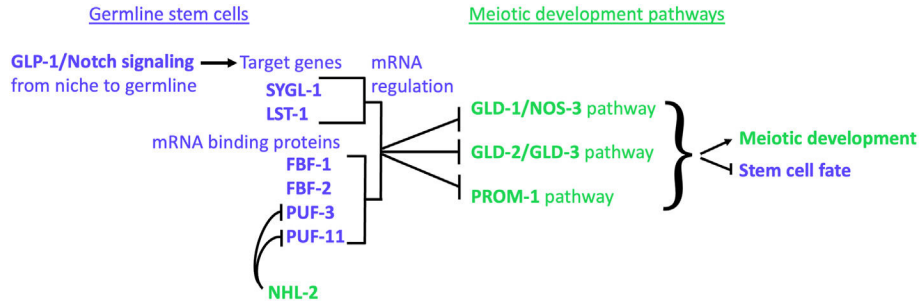


Fig. 9. Model for NHL-2 activity in the regulatory network controlling the germline stem cell fate versus meiotic development decision.

Our data support the model that NHL-2 limits PUF-3 and PUF-11 accumulation to promote the GSC fate/inhibit meiotic entry (also see Fig. 1). NHL-2 may also downregulate the activity of other members of the PUF hub, FBF-1 and FBF-2. ALG-5 and CGH-1 were also found to promote the stem cell fate/inhibit meiotic entry, possibly by acting with NHL-2 (not shown).

Author Manuscript

Author Manuscript

Author Manuscript

Author Manuscript

Table 1

Loss of *nhl-2* function suppresses the *glp-1(q224ts)* germline proliferation defect allowing production of embryos at 20 °C.

Genotype	N	No. embryos produced ^a ± SEM (range)
<i>glp-1(q224)</i>	20	0
<i>nhl-2(q162) glp-1(q224)</i>	10	124 ± 18 (46–182)
<i>nhl-2(ok818) glp-1(q224)</i>	9	112 ± 13 (56–180)
<i>alg-5(tm1163); glp-1(q224)</i>	11	8 ± 1.5 (1–18)
<i>alg-5(tm1163); nhl-2(ok818) glp-1(q224)</i>	19	117 ± 9 (0–166)

glp-1(q224ts) hermaphrodites grown at 15 °C produce offspring. When raised at 20 °C, they produce only a few sperm and no oocytes or embryos because all germ cells prematurely enter meiosis during early larval development. For the assays reported here, most strains were maintained at 15 °C, and L1 larvae were upshifted to 20 °C to assay for embryo production. The exception was *alg-5(tm1163); nhl-2(ok818) glp-1(q224)* animals, which were derived from *alg-5(tm1163); nhl-2(ok818) glp-1(q224)/hT2 glp* hermaphrodites grown at 20 °C. Results for *nhl-2(q162)* are consistent with Maine and Kimble (1993). N, number of individual hermaphrodites assayed.

^aEmbryos do not survive, indicating that the loss of NHL-2 function does not suppress *glp-1(ts)* maternal-effect embryonic lethality.